PHYSICAL REVIEW B VOLUME 44, NUMBER 14 1 OCTOBER 1991-II

V centers in $MgAl_2O_4$ spinels

A. Ibarra
EURATOM-CIEMAT Association, CIEMAT, Avenida Complutense 22, E-28040 Madrid, Spain

F. J. López
Departamento Fisica Aplicada (C-IV), Universidad Autónoma de Madrid, Cantoblanco, E-28049 Madrid, Spain

M. Jiménez de Castro*
EURATOM-CIEMAT Association, CIEMAT, Avenida Complutense 22, E-28040 Madrid, Spain

(Received 22 March 1991)

V centers induced by ionizing irradiation at 80 or 300 K in single-crystal and polycrystalline $MgAl_2O_4$ samples have been studied by use of electron paramagnetic resonance and optical absorption. V_t^- and V_o^{2-} centers, as a result of hole trapping at tetrahedral and octahedral cation vacancies, respectively, have been found to be responsible for two EPR bands centered at $g=2.011$ and optical absorption bands involved in the complex absorption spectrum at about 3.4 eV. These centers anneal thermally in a very wide step from 220 to 575 K.

I. INTRODUCTION

$MgAl_2O_4$ is a mixed oxide whose physical properties range between those of magnesium and aluminum oxide.[1] It is the most representative material of the wide family of chemical compounds with spinel crystalline structure that includes materials of important technological applications,[2,3] some of them being related to irradiation environment. In spite of this, there are only few papers dealing with the effect of ionizing radiation on these materials, particularly on $MgAl_2O_4$.

The spinel crystalline structure is a face-centered-cubic lattice of oxygen ions, with a lattice parameter of 8.08 Å for $MgAl_2O_4$.[4] Eight molecules form its unit cell, in which there are 64 tetrahedral symmetry sites and 32 octahedral ones. In the perfect case, which only occurs for $MgAl_2O_4$ from natural origin, magnesium ions occupy 8 tetrahedral positions and aluminum ions occupy 16 octahedral sites.[5] However, up to 30% of cation antisite disorder occurs in synthetic $MgAl_2O_4$ crystals.[6] This causes a very high concentration (up to hundreds of thousands ppm) of possible electron (Al^{3+} in tetrahedral symmetry sites) and hole (Mg^{2+} in octahedral symmetry sites) traps.

Besides this, $MgAl_2O_4$ always presents small stoichiometric deviations (some percents of Al excess) due to the characteristics of the phase diagram of MgO and Al_2O_3 mixtures, inducing the presence of a high concentration (around tens of thousands ppm) of cationic vacancies for electric-charge compensation.[7,8]

The above-mentioned very large concentration of intrinsic lattice defects that exists in all as-grown synthetic $MgAl_2O_4$ crystals (this is not the case of other insulator oxides, such as MgO and Al_2O_3) can play an important role in the response of this material to ionizing irradiation. It is generally admitted that ionizing irradiation only induces changes in the electric-charge state of preexisting defects as impurities and cationic vacancies. *V*-type centers are formed by hole trapping at oxygen ions surrounding cation vacancies, as has been extensively studied in MgO and Al_2O_3. In the case of $MgAl_2O_4$, only octahedral cation vacancies have been proposed to be caused by the nonstoichiometry of crystals, from comparisons between x-ray-diffraction and nuclear-magnetic-resonance results with some calculations.[9,10] However, making again these calculations, taking also into account the cation disorder, shows that the above-mentioned experimental results agree with the simultaneous existence of both octahedral and tetrahedral cation vacancies.[11] Thus a variety of *V*-type centers can be expected to be formed in $MgAl_2O_4$.

Only a few optical-absorption and electron-paramagnetic-resonance (EPR) studies on *V* centers in $MgAl_2O_4$ neutron[12,13] and γ-ray[14,15] irradiated at room temperature have so far been made. A broad optical-absorption band at 3.2 eV has been correlated with *V* centers only from analogies with MgO and Al_2O_3. This band, which vanishes between 370 and 550 K, is composed by at least four bands at around 2.8, 3.1, 3.6, and 3.9 eV whose thermal stabilities are slightly different. Some of them have been associated with valence changes of several impurities.[12,13] On the other hand, ultraviolet-light illumination of neutron-irradiated samples induces an EPR structure of 16 bands at $g=2.0015$, which is slightly anisotropic and has been related either to *V*-type centers[16] or to *F* centers.[13]

In view of this unclear situation, which may arise from different sample origins (i.e., different stoichiometry, disorder degree, impurity content, etc.), or different types of irradiation, a detailed study of optical-absorption and EPR spectra induced by x-ray irradiation in two different types of $MgAl_2O_4$ samples has been made in order to characterize *V* centers in this material.

II. EXPERIMENTAL TECHNIQUES

Single-crystalline Union Carbide $MgAl_2O_4$ samples (labeled UC samples), grown by the Czrochalski method, and polycrystalline Raytheon (Lexington, MA) samples (labeled *R* samples), fabricated by the fusion casting method,[17] have been used. The first ones were cut from a cylinder whose axis was parallel to the ⟨110⟩ crystalline axis. The last ones were kindly supplied by Dr. R. Heidinger (Kerforschungszentrum Karlsruhe, GFR). X-ray fluorescence and chemical analysis have been, respectively, used to know their stoichiometry and impurity contents. The results can be found in Table I.

The samples were x-ray irradiated at about 0.2 Mrad h^{-1} with a Siemens Kristalloflex 2H equipment with a tungsten anode tube. A ^{60}Co source was used for some γ irradiations at 3.9 Mrad h^{-1}. The same results were obtained as for x-ray irradiation.

EPR spectra were obtained with a Varian E-12 spectrometer working in the *X* band. The sample ($2\times2\times10$ mm^3) is placed in the center of the resonant cavity using a fused silica tube 4 mm in diameter. The sample temperature can be varied with a Varian E-257 variable-temperature accessory. Accurate values of the microwave frequencies and magnetic fields were obtained with a Hewlett-Packard HP5342A frequency meter and a Bruker ER 035 M gaussmeter, respectively. All spectra were measured with a modulation frequency of 100 kHz and a modulation amplitude of 0.5 G.

Optical-absorption measurements were made with a Cary 17 spectrophotometer. A small cryostat designed to be inserted in its measuring cell was used for low-temperature studies. The sample temperature can be varied between 90 and 400 K with a small oven attached to the sample holder. Optical bleaching of the x-ray-induced EPR optical-absorption bands have been made by illuminating the samples at several wavelengths with a calibrated 450-W Xe lamp through a Bausch and Lomb monochromator (high-intensity model).

III. RESULTS

A. Electron paramagnetic resonance

As-received UC samples show weak-intensity spectra which coincide with those reported for Mn^{2+} ions[18,19] and Cr^{3+} ions.[20,21] The intensity of the Cr^{3+} EPR spectrum vanishes when irradiating at 300 K, and its thermal recovery occurs between 300 and 700 K. The height of the Mn^{2+} bands does not change neither with x-ray irradiation nor after heating up to 800 K. The *R*-type samples do not show any EPR signal in as-received condition.

X-ray irradiation at 300 K induces in the UC single crystals a new spectrum at $g=2.011\pm0.001$, which is plotted in Fig. 1. It has a very high intensity, about 1000 times higher than any of those appearing before irradiation. This spectrum has been ascertained to be composed

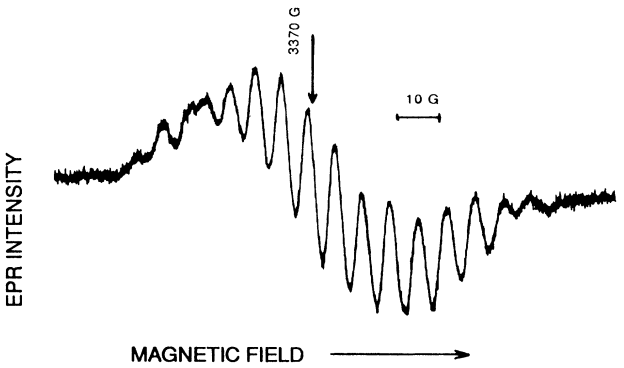

FIG. 1. EPR spectrum induced in UC $MgAl_2O_4$ by x-ray irradiation up to 650 krad at 300 K.

by two superimposed bands, a wide structureless one (labeled EPR-1) and another one (labeled EPR-2), which is a set of 13–16 (depending on sample orientation) very sharp lines. The second one is a pattern typically associated with hyperfine interactions. Only a slight sharpening of the whole set of bands is observed when measuring at 90 K a sample x-ray irradiated at 300 K.

The dependence on the microwave power used to excite the cavity, of the EPR-1 and EPR-2 band intensities, are plotted in Fig. 2. Here the shape of the EPR-1 band, to know its intensity, has been obtained from the middle points of all bands of the EPR-2 structure. Measurements have been made at 90 K (results at 300 K are very similar, but the necessary power to saturate the EPR-1 band is much higher). From Fig. 2 it is clear that each band behaves in a different way, thus indicating that they are associated with two different defects. This conclusion is also supported by the x-ray dose dependence at 300 K of the intensities of both EPR bands (see Fig. 3).

The number of lines observed in the EPR-2 structure (between 13 and 16), their separation (from 5.5 to 7.0 G), and the total spread (between 80 and 94 G at 300 K) depend on the sample orientation with a period of 180° for sample rotation around the ⟨110⟩ axis. A similar behavior is observed for the total spread of the EPR-1 structure. The peak-to-peak (p.-p.) width of each component of the EPR-2 structure ranges between 2 and 4 G. Those at the center are wider than those appearing at both sides. The separation between the components at the center is slightly different than at each side, this being either higher or lower than the other depending on the sample orientation. There is also an orientation dependence of the apparent band heights in the EPR-2 structure. Finally, there is a clear correlation between the observed number of components and the total structure width: This one is minimum when only 13 or 14 components appear, and it reaches a maximum when 15 or 16

TABLE I. Stoichiometry [*x* in $MgOx(Al_2O_3)$] and main impurity content (ppm) of $MgAl_2O_4$ samples.

Sample type	*x*	Fe	Ti	Cr	Mn	V
UC	1.02	100	50	<20	10	10
R	1.1	35	30	<20		

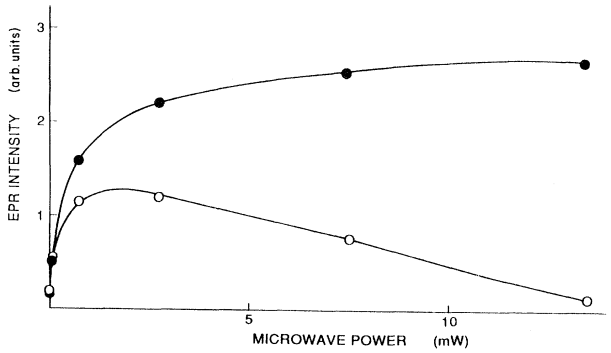

FIG. 2. Dependence on the microwave power of the intensities of the EPR-1 (●) and EPR-2 (○) bands x-ray induced at 300 K and measured at 90 K.

components are observed.

The same EPR spectrum is induced by x-ray irradiation at 90 K. Its intensity is about 2.5 times higher than that obtained by x-ray irradiation at 300 K. This was also observed in optical-absorption measurements.

Room-temperature optical bleaching of the x-ray-induced EPR bands has been made. For incident photon energies between 3 and 5 eV, the intensity of both EPR-1 and EPR-2 bands decreases in a similar proportion. No other of their characteristics changes by illumination. The bleaching efficiency is highest for a photon energy of about 3.9 eV.

The thermal stability of defects associated with the EPR spectra induced at 90 K has also been studied by a pulse thermal-annealing method. After heating the sample up to a given temperature value where it is maintained for 3 min, it is cooled rapidly down to 90 K for EPR measurements. Results can be found in Fig. 4. The intensities of both EPR-1 and EPR-2 structures are constant up to 210 K. Then they slowly anneal out up to about 575 K.

Polycrystalline *R* samples show the same x-ray-induced EPR spectrum as single crystals. Its height, position, and width are the same in both types of samples, although the hyperfine structure is weaker; it has only 15 components and does not obviously present any angular dependence.

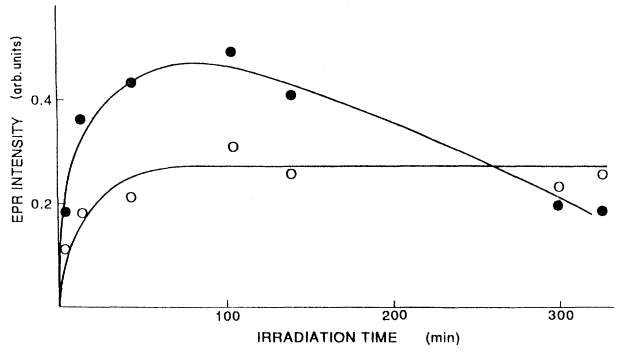

FIG. 3. Dependence on dose of the intensities of the EPR-1 (●) and EPR-2 (○) bands induced by x-ray irradiation at 300 K.

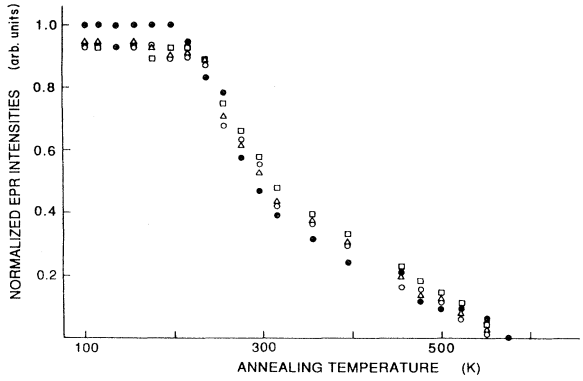

FIG. 4. Annealing curves for the EPR intensities: EPR-1 (●), side bands at low (△) and high (□) magnetic fields as well as central band (○) of the EPR-2 hyperfine structure.

B. Optical absorption

As-grown UC samples show two strong optical-absorption bands at 4.8 and 6.4 eV, probably related to Fe^{3+}-ion charge- transference processes,[14,22,23] and a very weak one at 0.62 eV, which could be due to tetrahedral Fe^{2+}.[24] As-received *R* samples show a high-energy absorption tail between 4 and 6 eV with a shoulder at 5.3 eV, which might be related to *F* centers[25,26] that can be formed during fabrication depending on the growing conditions.[27,28]

Figure 5 shows the changes in the absorption spectra of different samples induced by x-ray irradiation at 300 K. The differences between the optical-absorption spectra after and before irradiation have been plotted in this figure. As can be seen, a broadband peaked at around 3.4 eV appears. It is clearly composed of several strongly overlapped bands. There are some differences between the absorption spectra of the two different sample types, which may be due to the different relative heights of their components. Components at about 2.7, 3.4, 3.8, 5.0, and 4.8 eV in UC samples and at about 3.4, 3.8, and 5.0 eV in *R* samples appear in their x-ray-induced spectra.

The change in the absorption spectrum of UC samples induced by x-ray irradiation at 90 K can also be seen in Fig. 5. Besides a broadband at 3.4 eV, two others at about 5.7 and 6.2 eV also appear. The 3.4-eV-band amplitude is larger than that produced at 300 K at the same x-ray-irradiation dose, when this last one is also measured at 90 K.

A saturating growth of the optical-absorption-band heights with increasing dose is observed at 90 and 300 K, as can be seen in Fig. 6 for the 3.4-eV band in UC samples. However, the dose-saturation value is larger at 90 K. A similar behavior is found to occur in *R* samples.

The composed structure of the 3.4-eV band is again demonstrated by optical bleaching experiments, by measuring the changes induced by illumination with light at different wavelengths in the optical-absorption spectrum of an x-ray-irradiated sample. X-ray irradiations, light illuminations, and absorption measurements have

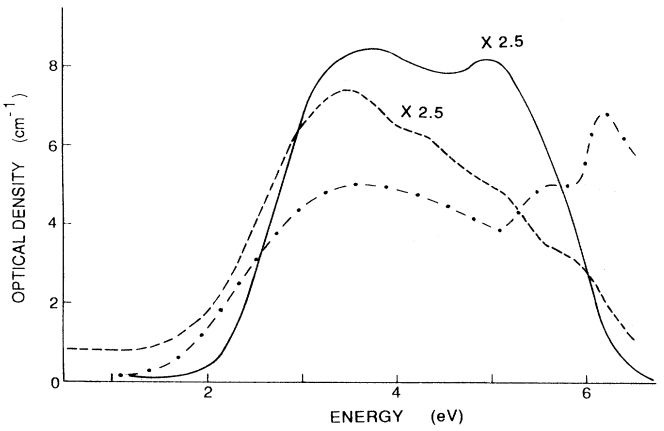

FIG. 5. Change in the absorption spectrum of $MgAl_2O_4$ induced by x-ray irradiation (dose around 650 krad) at 300 K: UC (dashed curve) and *R* (solid curve) samples, and at 90 K for UC samples (dot-dashed curve).

been made at 90 K, and the results are plotted in Fig. 7. In this figure the differences between the optical-absorption spectra taken before and after illuminations in samples previously x irradiated are shown. Light with energy below 3 eV does not induce any change, whereas illumination with light of energy between 3 and 5 eV causes a decrease in the height of the composed band at about 3.4 eV. This decrease is not uniform in the whole structure, but is more pronounced at energies nearby that of the incident light, and so it seems possible to make optical bleaching selectively on each of the different components of the 3.4-eV band.

The bleaching efficiency, as a function of the incident photon energy, is shown in the inset of this figure. This efficiency corresponds to the maximum optical-density change induced by illumination divided by the number of incident photons. It shows a maximum at around 4 eV. This agrees with previous results at room temperature in neutron-irradiated samples.[8]

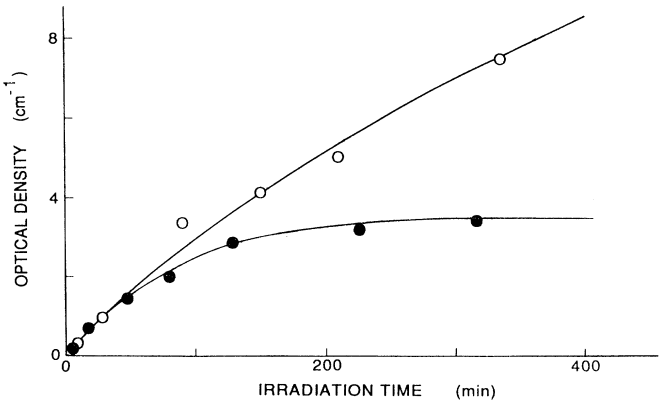

FIG. 6. Dependence on dose of the 3.4-eV optical-absorption-band height in UC samples, by x-ray irradiation at 90 K (○) and 300 K (●).

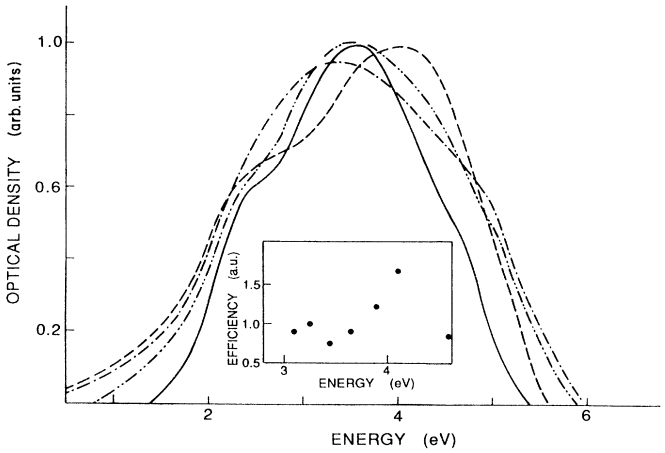

FIG. 7. Difference between the optical-absorption spectra taken before and after light illumination at 90 K at 4.1 eV (solid curve), 3.65 eV (dashed curve), 3.45 eV (double-dot-dashed curve), and 3.25 eV (dot-dashed curve) in a sample previously x-ray irradiated at 90 K. All spectra have been normalized to their maximum height. The inset shows the efficiency of this optical bleaching as a function of the incident photon energy.

The same pulsed thermal-annealing method as in EPR measurements has also been used to study the thermal stability of the absorption bands induced by irradiation at 90 K. Some of the obtained results are shown in Fig. 8. The height of the composed band at 3.4 eV does not vary between 90 and 220 K, although a small decrease is observed in this temperature range at 2.7 eV. From this temperature, all components of the 3.4-eV absorption band slowly decrease in a similar way up to around 570 K, as can be also seen in Fig. 9, where the optical densities at 2.7 and 3.4 eV have been plotted against the annealing temperature. They show a close parallelism with the thermal behavior of EPR-1 and EPR-2 bands. The

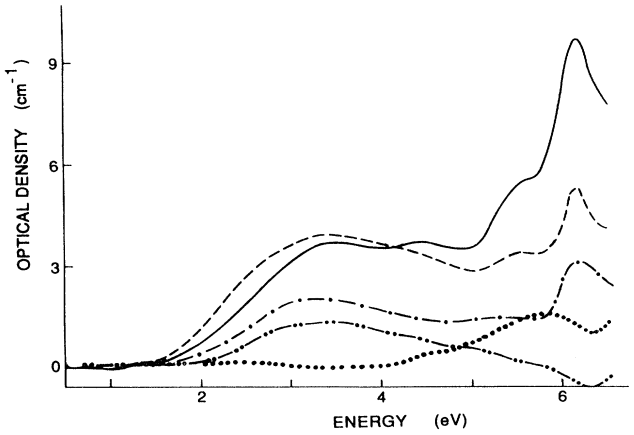

FIG. 8. Optical-absorption spectra of $MgAl_2O_4$ (UC samples) measured at 90 K after x-ray irradiation at this temperature followed by a heating pulse up to 100 K (dashed curve), 210 K (solid curve), 270 K (dot-dashed curve), 400 K (double-dot-dashed-curve), and 575 K (dotted curve).

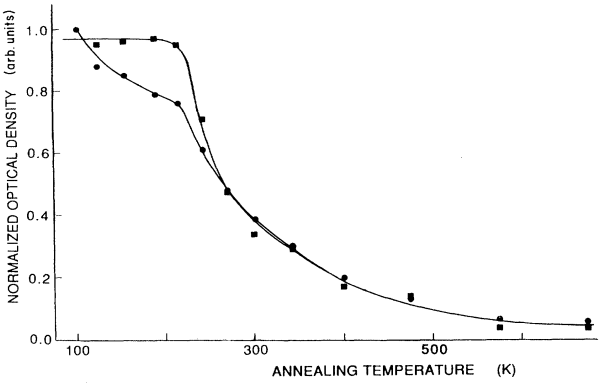

FIG. 9. Annealing curves for the optical-absorption bands at 2.7 eV (●) and 3.3 eV (■) in $MgAl_2O_4$ UC samples after x-ray irradiation at 90 K.

behavior of the 5.7- and 6.2-eV optical-absorption bands is different from the 3.4-eV one: They show increasing and decreasing stages along the pulsed thermal-annealing experiment, as indicated in Fig. 8. These bands will not be discussed any further in this work.

Polycrystalline *R* samples behave in a similar way as UC single crystals, although they have not been studied in such a detailed way.

IV. DISCUSSION

Both the EPR-1 and EPR-2 bands induced by x-ray irradiation in $MgAl_2O_4$ show different dose and microwave power dependences; thus they have to be associated with different centers, as was discussed above. Nevertheless, both appear at the same *g* value and have the same total width as well as similar optical and thermal stability, and so these centers must be closely related one to the other.

The characteristic height distribution of the 16 lines of the EPR-2 structure at $g=2.011$ corresponds to a typical hyperfine (hf) interaction between a $\frac{1}{2}$ electronic spin and three equivalent $\frac{5}{2}$ nuclear spins. Because of the very high EPR signal intensity, it is reasonable to assume that there is a very high concentration of centers responsible for it. This disregards impurities being involved, since the total impurity content is about only 100 ppm. On the other hand, both aluminum and magnesium have isotopes with nuclear spin $\frac{5}{2}$: ^{27}Al and ^{25}Mg. ^{27}Al is much more abundant (100%) than ^{25}Mg (10.1%) and its nuclear magnetic moment is higher (3.6385) than that of ^{25}Mg (0.8545).[29] Therefore, it seems sensible to conclude that the three $\frac{5}{2}$-nuclear-spin ions which interact with the electronic spin $\frac{1}{2}$ are aluminum ions. Since the EPR-2 structure is induced by ionizing irradiation, the electronic spin is expected to be a charge carrier which has been trapped by a preexisting latticed defect. The cation disorder and nonstoichiometry of $MgAl_2O_4$ samples provide a huge quantity of lattice defects which may serve as trapping centers. Among these are (i) aluminum and magnesium vacancies (leading to *V* centers by hole trapping), (ii) Mg^{2+} ions at Al^{3+} sites (which can act as hole traps), (iii) Al^{3+} ions at Mg^{2+} sites (possible electron traps), and (iv) oxygen vacancies (leading to *F*-type centers by electron trapping). Possibilities (ii) and (iii) can be disregarded as being the origin of the EPR-2 structure because there are more than three equidistant Al nuclei around them. Moreover, in oxides, it has been proposed[30] that the charge carriers must be trapped near double (or more) charged defects in order for the charge carrier to be poorly localized, thus allowing it to interact with the surrounding nuclei leading to the hf structure. On the other hand, possibility (iv) can also be neglected since the optical-absorption bands of *F*-centers[25,26] have not been observed to be induced by x-ray irradiation. Therefore, it is reasonable to conclude that the EPR-2 structure is related to hole trapping at cation vacancies, i.e., to *V*-type centers. The *g* value here obtained, higher than that associated with a free electron, supports this assignation. It is to be noted that a similar EPR band found in neutron-irradiation $MgAl_2O_4$ has also been ascribed to *V* centers.[16]

As for the concrete model for the center, there are in $MgAl_2O_4$ two possible defects involving a cation vacancy and three Al^{3+} ions, as is shown in Fig. 10. The indicated distances, taken from the literature,[4] have been obtained by x-ray-diffraction studies for a perfect stoichiometric crystal and without a nearby vacancy. If one of those centers traps a hole, it is expected that the O^{2-} ion becomes an O^- ion as in single oxides. In the case of the *a*-type defect, the cation vacancy will displace the O^- ion along the ⟨111⟩ axis, the three Al-O distances becoming smaller in the same degree, so that the three Al nuclei are equivalent. In the case of the *b*-type

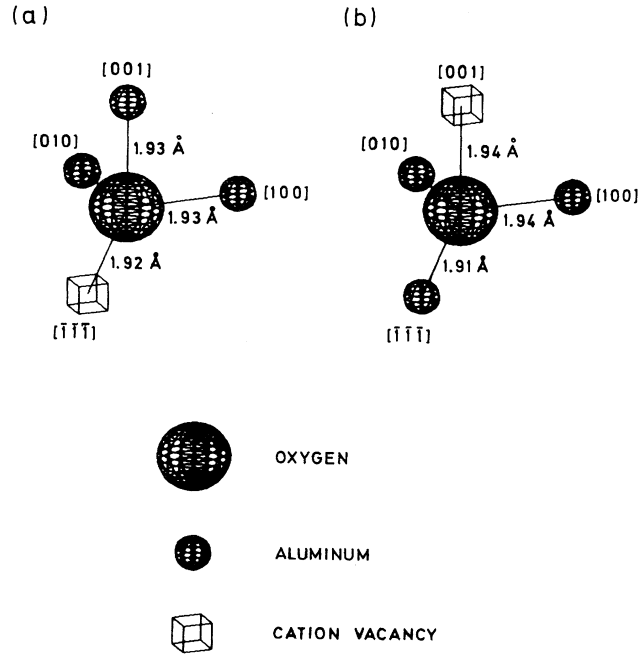

FIG. 10. Two possible surroundings of an oxygen ion in $MgAl_2O_4$, which include three Al^{3+} ions and a cation vacancy.

defect, this displacement will take place along a less clearly determined direction, this depending on whether the vacancy position is [100], [010], or [001]; now there are two equivalent and one nonequivalent nuclei. A defect of *a*-type with a trapped hole is a *V* center based on a cation vacancy with tetrahedral symmetry, and so in the usual nomenclature it should be labeled V_t^- center. The *b*-type center with a hole trapped is a *V* center based on a octahedrally coordinated vacancy, and so it would be a V_o^{2-} center. This last one is a defect associated with the structural disorder because it requires the presence of an aluminum ion in sites of tetrahedral coordination. According to these arguments, it seems reasonable to attribute the EPR-2 structure to only one type of these defects; otherwise it would have not been observed in polycrystalline *R* samples, due to the superposition of different spectra. This defect must be the V_t^- center because the hf pattern with 16 lines has to be associated to the presence of three equivalent Al nuclei.

The interaction between the magnetic electrons and the oxygen nuclei may be described by adding a term $\sum_i \mathbf{I}^i \cdot \hat{A}^i \cdot \mathbf{S}$ to the spin Hamiltonian.[31] Thus the hf lines occur at fields displaced from the zero interaction by

$$\partial H = \sum_i \mathbf{I}^i{}_z [A^i{}_s + A^i{}_p (3\cos^2\phi_i - 1)] ,$$

where $A^i{}_s$ represents the isotropic hf interaction due to electrons and $A^i{}_p$ the anisotropic hf interaction due to the *p* electrons as well as the dipole- dipole interaction for the *i* ligand, ϕ being the angle between the direction of the *i* bond and magnetic field. The observed weak angular dependence indicates that the $A^i{}_p$ anisotropic terms are much smaller, even not negligible, than the $A^i{}_s$ isotropic ones. This is also the behavior observed for the aluminum hf interactions of the Al-O-trapped hole center in a number of different oxides containing Al ions either as a constituent or as an impurity.[32] The hf interaction in the case of three nuclei at the same distance and weak anisotropy term produces a complex structure depending on the orientation whose envelope looks like a set of 15 or 16 bands,[11] and the apparent intensity of the central bands varies, with the orientation, from higher to lower than that of the extreme ones. This also justifies the detection of the EPR-2 structure in the polycrystalline *R* samples. It must be noted that in the Al-O hole centers mentioned above,[32] an almost exponential dependence on the Al-O distance of the $A^i{}_s$ coefficients has been observed. The value obtained from the EPR-2 structure (around 6.5 G) agrees very well with the predicted one (7 G) for a center with Al-O distance around 1.93 Å.[32]

The EPR-1 band must arise from a center of similar characteristics as those of the V_t^- center, since they have the same *g* value and the optical bleaching and thermal annealing of both EPR bands are very similar. Hole trapping at *b*-type defects, leading to V_o^{2-} centers, would be a good candidate. The two Al nuclei at the same distance and the one at different distance would produce a hf pattern with a minimum of $11 \times 6 = 66$ lines for each position of the vacancy, depending on the orientation of the sample. Therefore, only the envelope of that complex structure would be observed. V_t^- centers highly perturbed by nearby defects, as impurities or those caused by the antisite disorder, could also contribute to this resonance.

The dose dependence and optical and thermal stability of x-ray-induced optical-absorption bands at 3.4 eV are very similar to those of both EPR bands; therefore, the former can also be ascribed to different *V*-type centers. This agrees with previous similar ascriptions, only based on the similarities with other oxides, such as MgO and Al_2O_3.[14,15] In these oxides, unperturbed as well as impurity-perturbed *V*-type centers give rise to a complex optical-absorption spectrum in the visible region due to the overlapping of several bands.[33,34] However, it should be pointed out that not all components of the 3.4-eV broad absorption band may be due to *V* centers. Other hole-trapped centers, as, for example, $[Mg]^0_{Al}$, whose optical-absorption spectra are unknown, could also absorb in this region. More work is on the way to establish a clearer correlation among EPR and optical-absorption bands.

Results obtained so far by other authors in $MgAl_2O_4$ γ irradiated at room temperature indicate that the *V*-center optical-absorption bands are thermally stable up to 350 K and vanish at around 550 K.[14,15] Our EPR and optical-absorption results clearly indicate that *V* centers become thermally unstable at 220 K and their thermal- annealing range extends up to 575 K. This is in contrast with MgO and Al_2O_3, in which annealing of *V* centers occurs in a much narrower step.[34,35] An explanation for this very long annihilation process based on the dissolution of defect precipitates is not reasonable since it assumes aggregate formation by ionizing irradiation. Another possibility would be this annealing step being actually the sum of several individual annealing processes, one for each type of *V* center, as occurs in MgO and Al_2O_3 due to hole release. This must also be disregarded because the thermal annealing of the EPR-2 structure also takes place between 220 and 575 K, and it has been related to only one type of *V* center. Finally, a third model to explain this result requires that the defect acting as a trap from which charge carriers are thermally released has a very high retrapping probability. This may be accounted for if there is a very high concentration of trapping centers as compared with that of recombination centers, thus allowing the released charge carriers to be retrapped many times before recombination. Then the annihilation of trapping and recombination centers would take a long time. Recent thermoluminescence results support this conclusion, also indicating that *V* centers act as recombination centers for thermally released electrons in the whole temperature range between 220 and 575 K.[36]

Finally, it should be pointed out that our EPR results confirm that tetrahedral coordination vacancies are also present in synthetic $MgAl_2O_4$ samples, as was previously deduced from our calculations referred to in the Introduction.

*Present address: Instituto Ciencia de Materiales, Sede D, CSIC, Serrano 113, E-28006 Madrid, Spain.

[1]*Handbook of Chemistry and Physics,* 63rd ed., edited by R. C. Weast and M. J. Astle (CRC, Boca Raton, 1982).

[2]J. E. A. Maurits and A. M. Hawley, in *Advances in X-Ray Analysis,* edited by K. Heinrich *et al.* (Plenum, New York, 1972), Vol. 5.

[3]I. Wynn Jones and L. J. Miles, Proc. Br. Ceram. Soc. **19**, 161 (1971).

[4]T. J. Gray, in *High Temperature Oxides,* edited by A. M. Alper (Academic, New York, 1971), Pt. IV.

[5]G. E. Bacon, Acta Crystallogr. **5**, 684 (1952).

[6]V. Schmocker, H. R. Boesch, and F. Waldner, Phys. Lett. **40A**, 237 (1972).

[7]F. Colin, Rev. Int. Hautes Temp. Refract. **5**, 269 (1968).

[8]L. S. Cain, G. J. Pogatshnik, and Y. Chen, Phys. Rev. B **37**, 2645 (1988).

[9]H. Jagodzinski and H. Saalfield, Z. Kristallogr. **110**, 197 (1958).

[10]R. Dupree, M. H. Lewis, and M. E. Smith, Philos. Mag. A **53**, L17 (1986).

[11]A. Ibarra, R. Vila, and M. Jiménez de Castro, Philos. Mag. Lett. (to be published).

[12]T. I. Voitsenya, V. T. Gritsyna, V. B. Kol'ner, T. I. Korneeva, and L. A. Litninov, Neorg. Mater. **16**, 2580 (1980).

[13]V. T. Gritsyna, T. I. Voitsenya, T. I. Korneeva, V. B. Kol'ner, and A. M. Pshisukha. Zh. Tekh. Fiz. **50**, 2220 (1980) [Sov. Phys. Tech. Phys. **25**, 1294 (1980)].

[14]G. S. White, K. H. Lee, and J. H. Crawford, Jr., Phys. Status Solidi A **42**, K127 (1977).

[15]G. S. White, R. V. Jones, and J. H. Crawford, Jr., J. Appl. Phys. **53**, 265 (1982).

[16]V. T. Gritsyna and V. A. Kobyakov, Zh. Tekh. Fiz. **55**, 354 (1985) [Sov. Phys. Tech. Phys. **30**, 206 (1985)].

[17]R. L. Gentilman, Ceram. Bull. **60**, 906 (1981).

[18]F. Waldner, Helv. Phys. Acta **35**, 756 (1962).

[19]J. S. Shaffer, H. A. Farach, and C. P. Poole, Jr., Phys. Rev. B **13**, 1869 (1976).

[20]R. Stahl-Brade and W. Low, Phys. Rev. **116**, 561 (1959).

[21]V. A. Atsarkin, Zh. Eksp. Teor. Fiz. **43**, 839 (1962) [Sov. Phys. JETP **16**, 593 (1963)].

[22]G. A. Slack, F. S. Ham, and R. M. Chrenko, Phys. Rev. **152**, 376 (1966).

[23]C. Ballesteros, L. S. Cain, S. J. Pennycock, R. Gonzalez, and Y. Chen, Philos. Mag. A **59**, 907 (1989).

[24]G. A. Slack, Phys. Rev. **134**, A1268 (1964).

[25]G. P. Summers, G. S. White, K. H. Lee, and J. H. Crawford, Jr., Phys. Rev. B **21**, 2578 (1980).

[26]J. M. Bunch, Phys. Rev. B **16**, 724 (1977).

[27]V. T. Gritsyna, T. A. Bazilevskaya, and V. B. Kol'ner, Neorg. Mater. **23**, 112 (1987).

[28]G. S. White, K. H. Lee, and J. H. Crawford, Jr., Appl. Phys. Lett. **35**, 1 (1979).

[29]See, for instance, *Handbook of Chemistry and Physics,* edited by R. C. Weast (CRC, Cleveland, 1971).

[30]N. Y. Konstantinov, L. V. Karaseva, and V. V. Gromov, Dokl. Adad. Nauk. SSSR **228**, 631 (1980).

[31]S. Ogawa, J. Phys. Soc. Jpn. **15**, 1474 (1960).

[32]F. J. Adrian, A. N. Jette, and J. M. Spaeth, Phys. Rev. B **31**, 3923 (1985).

[33]Y. Chen and W. A. Sibley, Phys. Rev. **154**, 842 (1967).

[34]T. J. Turner and J. H. Crawford, Jr., Solid State Commun. **17**, 167 (1975).

[35]M. M. Abraham, W. P. Unruh, and Y. Chen, Phys. Rev. B **10**, 3539 (1974).

[36]A. Ibarra, F. Mariani, R. Serna, J. Mollá, and M. Jiménez de Castro, Radiation Effects and Defects in Solids (to be published).